Nanoclusters

Deutsche Ausgabe: DOI: 10.1002/ange.201609144
Internationale Ausgabe: DOI: 10.1002/anie.201609144

# Site Preference in Multimetallic Nanoclusters: Incorporation of Alkali Metal Ions or Copper Atoms into the Alkynyl-Protected Body-Centered Cubic Cluster $[Au_7Ag_8(C{\equiv}C^tBu)_{12}]^+$

*Yu Wang[+], Haifeng Su[+], Liting Ren[+], Sami Malola, Shuichao Lin, Boon K. Teo,* Hannu Häkkinen,* and Nanfeng Zheng**

*Dedicated to Professor Galen D. Stucky on the occasion of his 80th birthday*

***Abstract:*** *The synthesis, structure, substitution chemistry, and optical properties of the gold-centered cubic monocationic cluster $[Au@Ag_8@Au_6(C{\equiv}C^tBu)_{12}]^+$ are reported. The metal framework of this cluster can be described as a fragment of a body-centered cubic (bcc) lattice with the silver and gold atoms occupying the vertices and the body center of the cube, respectively. The incorporation of alkali metal atoms gave rise to $[M_nAg_{8-n}Au_7(C{\equiv}C^tBu)_{12}]^+$ clusters ($n=1$ for $M=$ Na, K, Rb, Cs and $n=2$ for $M=$ K, Rb), with the alkali metal ion(s) presumably occupying the vertex site(s), whereas the incorporation of copper atoms produced $[Cu_nAg_8Au_{7-n}(C{\equiv}C^tBu)_{12}]^+$ clusters ($n=1$–6), with the Cu atom(s) presumably occupying the capping site(s). The parent cluster exhibited strong emission in the near-IR region ($\lambda_{max}=818$ nm) with a quantum yield of 2% upon excitation at $\lambda=482$ nm. Its photoluminescence was quenched upon substitution with a $Na^+$ ion. DFT calculations confirmed the superatom characteristics of the title compound and the sodium-substituted derivatives.*

Superatoms are a class of clusters that mimic the chemical nature of atoms in the periodic table.[1,2] In 1984, Knight and co-workers found that sodium clusters with electron counts of 2, 8, 20, 34, 40, or 58 were more abundant in mass analysis. They proposed a jellium model to describe the electronic shell structures of many metal clusters.[3] According to this model, the Aufbau principle of superatomic orbitals gives rise to electronic configurations of $1S^21P^61D^{10}2S^21F^{14}2P^61G^{18}$ and so on.[4–7] A wide variety of superatoms have been predicted and experimentally obtained.[8–15] Superatoms were first prepared as naked metal clusters in the gas phase. Recently, with the introduction of organic ligands as surface-stabilizing agents, a large number of Au/Ag nanoclusters have been successfully prepared by solution chemistry. Many of these clusters possess closed-shell electronic structures and can thus be considered as superatoms.[16–26] Alkali metals are similar to coinage metals in that they both have a valence-shell $s^1$ electronic configuration. It should therefore be possible to substitute alkali metal ions for coinage metals in metal nanoclusters. However, prior to this work, there were no reports on the incorporation of alkali metals into ligand-stabilized coinage-metal clusters. Moreover, coinage metals are known to adopt face-centered cubic (fcc) structures in the bulk phase, and their alloys such as electrum (a naturally occurring alloy of gold and silver) have randomly disordered Au/Ag arrangements. It is unclear whether there would be site preference for foreign atoms or ions upon doping into Au/Ag nanoclusters. These issues prompted us to synthesize and structurally characterize the title cluster $[AuAg_8Au_6(C{\equiv}C^tBu)_{12}]^+$ (**1**) and study its substitution chemistry, mass spectra (MS), and optical properties.

The title cluster **1** has a body-centered cubic (bcc) framework with an ordered $Au@Ag_8@Au_6$ multishell structure and is protected by twelve alkynyl ligands. It is closely related to the previously reported halide-centered hexacapped cubic silver alkynyl monocationic clusters $[Ag_{14}(C{\equiv}C^tBu)_{12}X]^+$ (**2**; X = F, Cl, Br).[27] The noncentered analogue is also known as a dicationic cluster $[Ag_{14}(C{\equiv}C^tBu)_{12}][BF_4]_2$ (**3**).[28] The title cluster **1** represents the basic building block of a bcc structure in the bulk phase. In addition to being strikingly different to the fcc structure of bulk coinage metals, the structure of **1** is also at odds with many gold and silver nanoclusters, which prefer icosahedral structures. **1** also bears a kinship to the gold nanocluster $[Au_{38}S_2(SR)_{20}]$ (**4**), which features two sulfido atoms and 20 adamantanethiolate ligands. Cluster **4** has been described as an incomplete and distorted version of a $3\times3\times2$ "cutout" of the bcc bulk phase.[29]

The site preference of foreign atoms or dopants in a nanocluster is a critical issue in metal cluster chemistry as well as in the design and fabrication of technologically important nanomaterials, such as bimetallic catalysts. There are three possible substitution sites for foreign atom(s) in

[*] Y. Wang,[+] Dr. H. F. Su,[+] L. T. Ren,[+] Dr. S. C. Lin, Prof. B. K. Teo, Prof. N. F. Zheng
Collaborative Innovation Center of Chemistry for Energy Materials
State Key Laboratory for Physical Chemistry of Solid Surfaces and Engineering Research Center for Nano-Preparation Technology of Fujian Province
College of Chemistry and Chemical Engineering
Xiamen University, Xiamen 361005 (China)
E-mail: boonkteo@xmu.edu.cn
nfzheng@xmu.edu.cn
Dr. S. Malola, Prof. H. Häkkinen
Departments of Physics and Chemistry
Nanoscience Center, University of Jyväskylä
Jyväskylä 40014 (Finland)
E-mail: hannu.j.hakkinen@jyu.fi
[+] These authors contributed equally to this work.

Supporting information for this article can be found under: http://dx.doi.org/10.1002/anie.201609144.

  

a hexacapped bcc cluster such as **1**: a) the body center, b) the eight vertices, and c) the six capping atoms on the square faces of the cube. (Note that the six capping atoms eventually become the centers of the six adjacent cubes in a bcc lattice.) As we shall see, we observed substitution at all of these sites in this work: Whereas the majority of the clusters reported herein are gold-centered, a parallel series of silver-centered clusters has also been observed as minor products in ESI-MS (Figure 3, see below). The substitution of one or two vertices of the cube by alkali-metal ions gave rise to $[M_nAg_{8-n}Au_7(C{\equiv}C^tBu)_{12}]^+$ (**5**) clusters (M = Na, K, Rb, Cs for $n=1$ (**5a**) and M = K, Rb for $n=2$ (**5b**)). On the other hand, successive substitution of the capping Au atoms by Cu produced $[Cu_nAg_8Au_{7-n}(C{\equiv}C^tBu)_{12}]^+$ (**6**) clusters ($n=1$–6) as revealed by ESI-MS and corroborated by DFT calculations.

The structure of **1** was determined by single-crystal X-ray diffraction (Figure 1 a).[30] The metal framework of the cluster has a core–shell–shell arrangement of $Au@Ag_8@Au_6$ (Figure 1 a). The eight Ag atoms form a Au-centered cube with Ag–Ag bond lengths in the range of 3.270–3.277 Å (avg. 3.273 Å), suggesting significant but somewhat weak Ag–Ag bonds within the $Ag_8$ cube. (For comparison, the average distances between adjacent Ag atoms in **2** (X = Cl) and **3** are significantly longer with 3.649 and 3.769 Å, respectively.) In contrast, the Au–Ag distances between the central Au atom and the $Ag_8$ cube range from 2.832 to 2.842 Å (avg. 2.835 Å), signifying much stronger Au–Ag bonding. The metal–metal distances in cluster **1** are consistent with those observed in organometallic clusters (2.8–3.2 Å).[31–33] Note that the average Au–Ag distance (1/2 of the body diagonal) of 2.835 Å is precisely $\sqrt{3}/2$ times the average Ag–Ag distance of 3.273 Å (the edge length of the cube), confirming that the gold atom is located at the geometrical center of the cube. Each of the six $Ag_4$ square faces of the $Ag_8$ cube is capped with one Au atom (Au–Ag: 2.914 Å (avg.)), forming a square pyramid and giving rise to the hexacapped cube. Furthermore, the Au and Ag atoms in **1** are arranged orderly in the multishell $Au@Ag_8@Au_6$ structure, in sharp contrast to the randomly distributed solid solution of the fcc bulk AuAg alloy. This ordered shell-by-shell structure is related to the site preference, which will be discussed later. We note that a bcc arrangement has also been reported for the 40 electron jellium cluster $SiAl_{14}(C_5H_5)_6$.[34,35] In this main-group cluster, a silicon atom is located at the center of an $Al_8$ cube, which is face-capped by six $Al(C_5H_5)$ moieties.

Each of the surface-capping Au atoms in **1** is linearly coordinated by two $^tBuC{\equiv}C^-$ (TBA) ligands, forming a $^tBuC{\equiv}C{-}Au{-}C{\equiv}C^tBu$ staple unit. Although the $RC{\equiv}C{-}Au{-}C{\equiv}CR$ motif resembles the RS–Au–SR staple motif, they have very different binding structures on metal surfaces. Whereas SR–Au–SR motifs typically bind to inner metal atoms via the sulfur atoms in the motifs, $RC{\equiv}C{-}Au{-}C{\equiv}CR$ motifs exhibit various coordination modes.[36,37] For instance, the 20 $PhC{\equiv}C^-$ ligands on the surface of $Au_{24}Ag_{20}(SPy)_4(PA)_{20}Cl_2$ exhibit five different coordination modes.[36] Sixteen of them serve as $\mu_3$-$\eta^1$(Au),$\eta^2$(Ag),$\eta^2$(Ag) or $\mu_3$-$\eta^1$(Au),$\eta^2$(Ag),$\eta^1$(Ag) or $\mu_3$-$\eta^1$-(Au),$\eta^2$(Ag) ligands, and the remaining four act as $\mu_2$-$\eta^1$(Au),$\eta^1$(Ag) or $\mu_2$-$\eta^1$(Au),$\eta^2$(Ag) ligands. In the case of **1**, all $^tBuC{\equiv}C^-$ ligands adopt the $\mu_3$-$\eta^1$(Au),$\eta^2$(Ag) mode.

The electrospray ionization mass spectrum (ESI-MS) of **1** (as prepared) is depicted in Figure 2 a. The high purity of the as-prepared product was confirmed by a single peak corresponding to monocationic $[Ag_8Au_7(TBA)_{12}]^+$ at $m/z$ 3214.8. An expansion of the ESI-MS peak also confirmed the Au versus Ag atomic distribution as determined by the overall mass and the $^{107}Ag/^{109}Ag$ isotope pattern (see the Supporting Information, Figure S2).

As **1** adopts the unusual bcc structure, we were curious whether other metals (especially those with a valence $s^1$ electron) adopting a bcc structure in their bulk phase (such as alkali metals) can be incorporated into the metal framework of **1**. It turned out that a sodium ion can be substituted for a Ag atom in **1**. Two different methods were used to incorporate $Na^+$ ions into **1**: reacting NaOMe with preformed

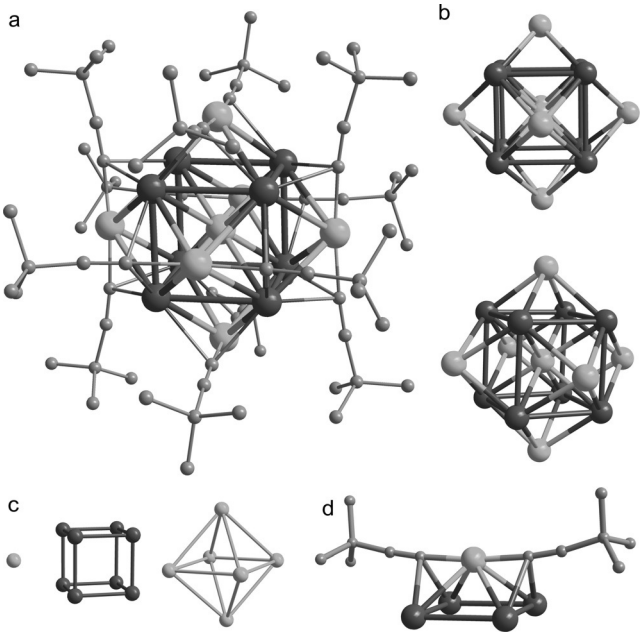


***Figure 1.*** The $[Au@Ag_8@Au_6(C{\equiv}C^tBu)_{12}]^+$ (**1**) monocation. a) Overall structure. b) Top and side views of the metal framework, $Au_7Ag_8$, showing the hexacapped bcc arrangement. c) Shell-by-shell representations of the metal framework, $Au@Ag_8@Au_6$ (note that the six capping Au atoms form an octahedron with no bonds between them). d) One of the six so-called $Au(C{\equiv}C^tBu)_2$ staple units capping a silver square of the $Ag_8$ cube. Ag black, Au light gray, C dark gray. Hydrogen atoms omitted for clarity.

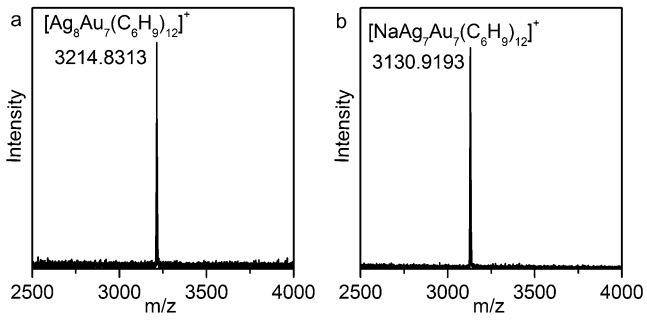


***Figure 2.*** ESI-MS spectra of the crude products **1** and **5a** in $CHCl_3$.

**1** or using NaOMe instead of $NEt_3$ in the preparation of **1**. Both methods produced a single peak corresponding to monocationic $[NaAg_7Au_7(TBA)_{12}]^+$ at $m/z$ 3130.9 in the ESI mass spectrum in the positive-ion mode (Figure 2b). Other alkali metals such as K, Rb, and Cs can also be likewise incorporated into **1**. When excess KOMe was used, $[KAg_7Au_7(TBA)_{12}]^+$ was formed, accompanied by a small amount of $[K_2Ag_6Au_7(TBA)_{12}]^+$ (Figure S3). Similar results were obtained when $Rb_2CO_3$ was used, except that half of the amount of **1** still remained after a long reaction time (Figure S4). The use of excess $Cs_2CO_3$ produced only $[CsAg_7Au_7(TBA)_{12}]^+$ (Figure S5).

The site preference of foreign atoms or dopants is an important issue in clusters. For Pd/Pt-exchanged $Au_{25}/Ag_{25}$ clusters stabilized by either phosphines or thiolates, the dopant atom prefers the center of the $Au_{13}/Ag_{13}$ core as the dopant (Pd, Pt) has a higher cohesive energy.[6,38–42] In fact, as early as in the 1990s, Teo and co-workers already demonstrated that foreign metal atoms (such as M = Pt, Pd, Ni) with higher cohesive energies than those of Au and Ag tend to occupy the icosahedral center(s) of vertex-sharing bi-icosahedral $Au_{12}Ag_{12}M$ and $Au_{11}Ag_{12}M_2$ clusters protected by phosphine and halide ligands.[6,7]

When copper was added during the synthesis of **1**, the capping gold atom(s), rather than silver, was/were replaced by copper atom(s). The ESI mass spectrum shows that up to six copper atoms can be substituted for the capping gold atoms in **1**, resulting in $[Cu_nAg_8Au_{7-n}(TBA)_{12}]^+$ (**6a**, $n = 1$–6 in Figure 3). A minor parallel silver-centered series, formulated as $[Cu_nAg_9Au_{6-n}(TBA)_{12}]^+$ (**6b**, $n' = 1$–5 in Figure 3), was also observed. We believe that the ninth Ag atom in **6b** resides at the center of the $Ag_8$ cube as the center is the nucleation site. An alternative structure for the parent cluster of the **6b** series, namely $[Ag_9Au_6(TBA)_{12}]^+$ (**6b,** $n' = 0$) would be a gold-centered $Ag_8$ cube capped with five $Au(TBA)_2$ and a $Ag(TBA)_2$ staple on the six square faces. The latter is thermodynamically less stable. The energy disparity stems from competition between the metal–metal bond energies (Au–Ag > Ag–Ag) and the metal–ligand bond energies (C–Au–C > C–Ag–C). The latter dominates. Hence, the minor parallel series **6b** may be written as $[Ag@Ag_8@Au_{6-n'}Cu_{n'}(TBA)_{12}]^+$, with only the clusters with $n' = 1$–5 having been observed. However, unlike for the reaction with alkali metals, reacting copper salts with preformed **1** did not result in the incorporation of Cu into **1**, presumably owing to the fact that the bonding between Au and $^t$BuC≡C$^-$ is much stronger than that between Cu and $^t$BuC≡C$^-$.

As shown in Figure 4a, **1** exhibits a broad multiband optical absorption in the UV/Vis region with three unresolved bands at 459, 483, and 510 nm. The absorption bands of **5a** (M = Na) are similar to those of **1**, indicating that $Na^+$ substitution does not affect the UV/Vis absorption. However, the modulation of the electronic structure has a significant effect on the photoluminescence of **1** (Figures 4b and S6). Cluster **1** strongly emits in the near-IR region ($\lambda_{max} = 818$ nm), with a quantum yield of 2% upon excitation at $\lambda = 482$ nm. In comparison, $[NaAg_7Au_7(TBA)_{12}]^+$ emits only weak photoluminescence with a quantum yield of 0.34% when excited at same frequency.

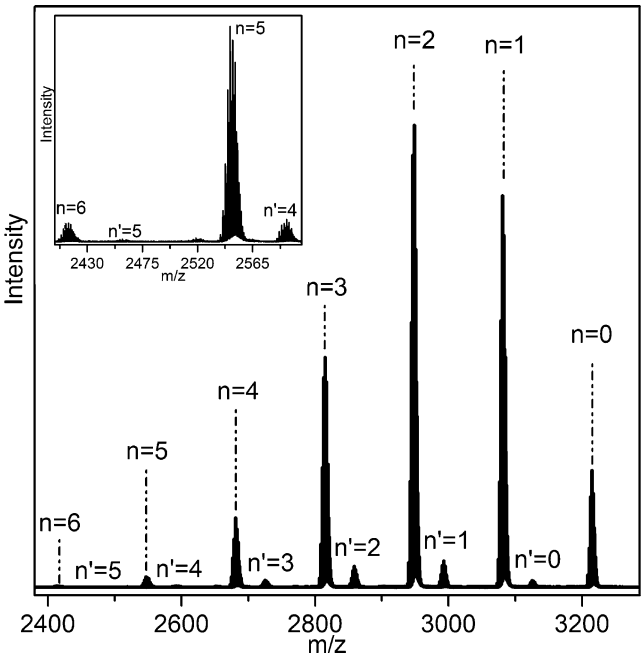


***Figure 3.*** ESI-MS spectra of the as-prepared product **6** showing the major gold-centered cubic cluster series $[Cu_nAg_8Au_{7-n}(TBA)_{12}]^+$ (**6a**, $n = 0$–6) along with the minor silver-centered cubic cluster series $[Cu_nAg_9Au_{6-n'}(TBA)_{12}]^+$ (**6b**, $n' = 0$–5). Inset: Magnification of the $m/z$ 2400–2600 region.

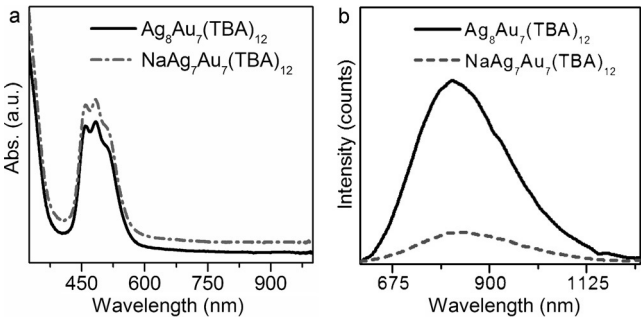


***Figure 4.*** UV/Vis and NIR photoluminescence ($\lambda_{ex} = 482$ nm) spectra of **1** (solid curves) and **5a** (dashed curves) in $CHCl_3$.

Density functional theory (DFT) calculations were carried out to analyze the electronic structures and optical absorption properties of **1** and the effect of $Na^+$ substitution. Analysis of the angular momentum character of the projected molecular orbitals of **1** revealed a jelliumatic shell closing at the HOMO state of 1S with two electrons and the LUMO state of 1P (Figure S7). This result is consistent with electron counting,[4–7] which gives 7 + 8 = 15 delocalized electrons from the metals, twelve of which are delocalized in the metal–ligand bonds, and one electron has to be deducted as the cluster complex is a cation. Thus the title cluster is a formerly 15–12–1 = 2 electron jelliumatic system. The HOMO–LUMO gap of **1** was calculated to be 1.86 eV.

The UV/Vis spectra of **1** and **5a** (M = Na) were also calculated (Figure S8). They agree reasonably well with the experimental ones (Figure 4a). UV/Vis spectra of **1** with

different overall charges ($q=0$, $+1$, and $+3$) were also calculated (Figure S9). Only $q=+1$ compares well with the experiment. However, the calculated bands at 391, 407, and 429 nm are located at somewhat higher energies than the experimentally observed ones at 459, 483, and 510 nm. The high-energy bands can be interpreted mainly as ligand-to-superatom and superatom-to-ligand transitions as shown in Figure S10. There is one additional band at lower energies, caused by superatom-to-superatom S-to-P state transition (Figure S10a).

To gain some insight as to why only up to two alkali metal atoms can be incorporated into **1**, the structures of $[Na_nAg_{8-n}Au_7(TBA)_{12}]^+$ ($n=0$–8) were optimized by DFT calculations (Figure S11 and Table S1). Comparisons of the calculated atomic charge distributions and total energies are provided in Tables S2 and S3, respectively. As shown in Table S2, the charges on the Na atoms are approximately $+0.86$, indicating that they are present as $Na^+$ ions in the cluster. For $n=2$, there are three possible sites for the two $Na^+$ ions in $[Na_2Ag_6Au_7(TBA)_{12}]^+$, namely along an edge, a face diagonal, or a body diagonal of the cube. As shown in Table S3, the isomer with the $Na^+$ ions on a body diagonal is most stable, and the isomer with the $Na^+$ ions on edges is the least stable. Based on our DFT calculations, it is reasonable to predict that the configuration with the alkali metal ions on a body diagonal will be the observed structure for all alkali metal (M) substituted $[M_2Ag_6Au_7(TBA)_{12}]^+$ clusters (**5b**).

For $n>2$, the additional $Na^+$ ions must be adjacent to other $Na^+$ ion(s), and the resulting strong Coulombic repulsions between neighboring $Na^+$ ions (along the cube edges) will increase the energetic cost for the addition of more alkali metal ions as each $Na^+$ ion bears a charge of $+0.86$ in comparison to the charge of $+0.43$ to $+0.47$ on each substituted Ag atom (see Table S2). Furthermore, each additional $Na^+$ ion adds about $0.86-0.43=0.43$ electrons to the metal cluster framework. The additional electron density is mainly "absorbed" by the Au atoms and the ligands. As listed in Table S2 (charge per atom or TBA), for $[Na_nAg_{8-n}Au_7(TBA)_{12}]$,$^+$ the central Au atom becomes substantially more negatively charged (from $-0.324$ to $-0.724$) while the other Au atoms (capping atoms) become less positively charged (from 0.201 to 0.090) as $n$ increases from 0 to 8 (successively replacing Ag by $Na^+$). Concomitantly, the TBA ligands become more negatively charged (from $-0.302$ to $-0.473$) while the Ag atoms become less positively charged (from 0.466 to 0.426) as $n$ increases from 0 to 7 ($n=8$ means a total replacement of all Ag atoms by Na ions). This, in a sense, is an "internal pseudo reduction" process with a limit that is probably reached at $n\approx 2$ under the present experimental reaction conditions.

DFT calculations (after geometry optimization) also showed that for $n=1$, the average Na–Au(caps) distance is 3.187 Å, and the average Na–Ag(cube) distance is 3.690 Å. The former is close to the sum of the atomic radius of a Na atom and the metallic radius of Au whereas the latter is extraordinarily long (i.e., lengthened by ca. 0.5 Å). Nevertheless, these values are comparable to the Rb–Au distance in bcc RbAu of 3.557 Å and the Cs–Au distance in bcc CsAu of 3.691 Å. In our computationally optimized clusters, the Na–Na distances between neighboring Na atoms are approximately 3.8–3.9 Å. These values are greater than the Na–Na distances in bulk Na metal (3.6 Å). We believe that these lengthening effects stem from the Coulombic repulsions described above.

In conclusion, a superatomic two-electron bimetallic nanocluster, $[AuAg_8Au_6(C{\equiv}C^tBu)_{12}]^+$, has been synthesized and structurally characterized. The structure of **1** is unique in two aspects: 1) The metal framework is a centered hexacapped cube, representing the basic building block of the body-centered cubic structure of the bulk phase (albeit with six neighboring body centers). 2) Instead of being randomly distributed, all eight silver atoms occupy the vertices of the cube, and all seven gold atoms occupy the body-center sites (one body center and six caps), forming a concentric three-shell $Au@Ag_8@Au_6$ structure. Alkali metal ions were incorporated into ligand-stabilized noble-metal nanoclusters for the first time. It was found that alkali metal ions prefer the vertex sites in **1** (replacing Ag atoms) as suggested by our DFT calculations whereas copper atoms prefer to replace the capping Au atoms (inferred from the MS data). The substitution of one of the cube vertices with a $Na^+$ ion quenches the photoluminescence of **1**. DFT calculations were also performed to determine as to why no more than two alkali metal ions could be incorporated into the structure of **1**. We hope that the successful incorporation of alkali metal ions and copper atoms into the title cluster will stimulate further work towards doping other metal clusters with foreign atoms or ions, thereby producing nanoclusters with novel structures and desirable properties, such as multimetallic nanocluster catalysts and magnetic superatoms.

## Experimental Section

Synthesis of **1**: $AuSMe_2Cl$ (6 mg) was first dissolved in a mixture of dichloromethane and methanol. $AgCH_3COO$ (5 mg) was added, and the reaction mixture was stirred for 5 min. Then, 50 μL $NEt_3$ and 10 μL *tert*-butylacetylene were added to the solution, which was stirred for 10 min. The reducing agent, *tert*-butylamine–borane (3.6 mg), was added to the mixture under vigorous stirring. The reaction mixture was stirred for 12 h at room temperature. The solution was centrifuged for 4 min at 14000 r min$^{-1}$. The brown supernatant was subjected to evaporation in the dark at room temperature. Red block crystals were obtained after 3 weeks (yield ca. 25% based on Au).

Synthesis of **5**: Method A: In the synthesis of **1** described above, NaOMe (5 mg) was substituted for $NEt_3$ while keeping the other conditions the same. Method B: A solution of NaOMe (10 mg) in methanol (1 mL) was added to a dichloromethane solution of **1** (3 mg of crystals of **1**). After stirring for 30 min, the solvents were removed on a rotary evaporator. The solid obtained was washed with methanol three times to remove excess NaOMe. The incorporation of other alkali metals into **1** was achieved by replacing NaOMe in method B with KOMe, $Rb_2CO_3$, or $Cs_2CO_3$.

Synthesis of copper-containing **6**: $AuSMe_2Cl$ (6 mg) was first dissolved in a mixture of dichloromethane and methanol. $AgCH_3COO$ (5 mg) and $Cu(CH_3COO)_2$ (1 mg) were added, and the resulting mixture was stirred for 5 min. Then, 50 μL of $NEt_3$ and 10 μL of *tert*-butylacetylene were added to the solution, which was then stirred for 10 min. The reducing agent, *tert*-butylamine–borane (3.6 mg), was added to the mixture under vigorous stirring. The reaction mixture was stirred for 12 h at room temperature.

  

## Acknowledgements

We thank the MOST of China (2015CB932303) and the NSFC of China (21420102001, 21131005, 21390390, 21227001, 21333008) for financial support. B.K.T. acknowledges financial support from iChEM, Xiamen University. The work at the University of Jyväskylä was supported by the Academy of Finland (projects 266492, 294217 and Academy Professorship to H.H.). The computations were carried out at the CSC computing center in Espoo, Finland.

**Keywords:** alkali metals · alkynes · doping · nanoclusters · superatoms

**How to cite:** *Angew. Chem. Int. Ed.* **2016**, *55*, 15152–15156
*Angew. Chem.* **2016**, *128*, 15376–15380

[1] S. N. Khanna, P. Jena, *Phys. Rev. Lett.* **1992**, *69*, 1664–1667.
[2] S. N. Khanna, P. Jena, *Phys. Rev. B* **1995**, *51*, 13705–13716.
[3] W. D. Knight, K. Clemenger, W. A. Deheer, W. A. Saunders, M. Y. Chou, M. L. Cohen, *Phys. Rev. Lett.* **1984**, *52*, 2141–2143.
[4] W. Ekardt, *Phys. Rev. B* **1984**, *29*, 1558–1564.
[5] M. Walter, J. Akola, O. Lopez-Acevedo, P. D. Jadzinsky, G. Calero, C. J. Ackerson, R. L. Whetten, H. Gronbeck, H. Hakkinen, *Proc. Natl. Acad. Sci. USA* **2008**, *105*, 9157–9162.
[6] B. K. Teo, H. Zhang, *Coord. Chem. Rev.* **1995**, *143*, 611–636.
[7] H. Zhang, B. K. Teo, *Inorg. Chim. Acta* **1997**, *265*, 213–224.
[8] C. Ashman, S. N. Khanna, M. R. Pederson, *Phys. Rev. B* **2002**, *66*, 193408.
[9] D. E. Bergeron, A. W. Castleman, T. Morisato, S. N. Khanna, *Science* **2004**, *304*, 84–87.
[10] D. E. Bergeron, P. J. Roach, A. W. Castleman, N. Jones, S. N. Khanna, *Science* **2005**, *307*, 231–235.
[11] J. U. Reveles, S. N. Khanna, *Phys. Rev. B* **2006**, *74*, 035435.
[12] J. U. Reveles, S. N. Khanna, P. J. Roach, A. W. Castleman, Jr., *Proc. Natl. Acad. Sci. USA* **2006**, *103*, 18405–18410.
[13] D. E. Jiang, S. Dai, *Inorg. Chem.* **2009**, *48*, 2720–2722.
[14] J. U. Reveles, P. A. Clayborne, A. C. Reber, S. N. Khanna, K. Pradhan, P. Sen, M. R. Pederson, *Nat. Chem.* **2009**, *1*, 310–315.
[15] M. Walter, M. Moseler, *J. Phys. Chem. C* **2009**, *113*, 15834–15837.
[16] P. D. Jadzinsky, G. Calero, C. J. Ackerson, D. A. Bushnell, R. D. Kornberg, *Science* **2007**, *318*, 430–433.
[17] M. Z. Zhu, C. M. Aikens, F. J. Hollander, G. C. Schatz, R. C. Jin, *J. Am. Chem. Soc.* **2008**, *130*, 5883–5885.
[18] A. Desireddy, B. E. Conn, J. Guo, B. Yoon, R. N. Barnett, B. M. Monahan, K. Kirschbaum, W. P. Griffith, R. L. Whetten, U. Landman, T. P. Bigioni, *Nature* **2013**, *501*, 399–402.
[19] B. S. Gutrath, I. M. Oppel, O. Presly, I. Beljakov, V. Meded, W. Wenzel, U. Simon, *Angew. Chem. Int. Ed.* **2013**, *52*, 3529–3532; *Angew. Chem.* **2013**, *125*, 3614–3617.
[20] H. Y. Yang, Y. Wang, H. Q. Huang, L. Gell, L. Lehtovaara, S. Malola, H. Häkkinen, N. F. Zheng, *Nat. Commun.* **2013**, *4*, 2422.
[21] R. S. Dhayal, J. H. Liao, Y. C. Liu, M. H. Chiang, S. Kahlal, J. Y. Saillard, C. W. Liu, *Angew. Chem. Int. Ed.* **2015**, *54*, 3702–3706; *Angew. Chem.* **2015**, *127*, 3773–3777.
[22] K. Kwak, Q. Tang, M. Kim, D. E. Jiang, D. Lee, *J. Am. Chem. Soc.* **2015**, *137*, 10833–10840.
[23] L. W. Liao, S. M. Zhou, Y. F. Dai, L. Liu, C. H. Yao, C. F. Fu, J. L. Yang, Z. K. Wu, *J. Am. Chem. Soc.* **2015**, *137*, 9511–9514.
[24] X.-K. Wan, Q. Tang, S.-F. Yuan, D.-e. Jiang, Q.-M. Wang, *J. Am. Chem. Soc.* **2015**, *137*, 652–655.
[25] S. Wang, Y. Song, S. Jin, X. Liu, J. Zhang, Y. Pei, X. Meng, M. Chen, P. Li, M. Z. Zhu, *J. Am. Chem. Soc.* **2015**, *137*, 4018–4021.
[26] C. H. Yao, Y. J. Lin, J. Y. Yuan, L. W. Liao, M. Zhu, L. H. Weng, J. L. Yang, Z. K. Wu, *J. Am. Chem. Soc.* **2015**, *137*, 15350–15353.
[27] D. Rais, J. Yau, D. M. P. Mingos, R. Vilar, A. J. P. White, D. J. Williams, *Angew. Chem. Int. Ed.* **2001**, *40*, 3464–3467; *Angew. Chem.* **2001**, *113*, 3572–3575.
[28] O. M. Abu-Salah, M. H. Ja'far, A. R. Al-Ohaly, K. A. Al-Farhan, H. S. Al-Enzi, O. V. Dolomanov, J. A. K. Howard, *Eur. J. Inorg. Chem.* **2006**, 2353–2356.
[29] C. Liu, T. Li, G. Li, K. Nobusada, C. J. Zeng, G. S. Pang, N. L. Rosi, R. C. Jin, *Angew. Chem. Int. Ed.* **2015**, *54*, 9826–9829; *Angew. Chem.* **2015**, *127*, 9964–9967.
[30] Crystal data for **1**: $C_{72}H_{108}Ag_8Au_7$, $a = b = 21.8325(8)$ Å, $c = 15.4322(5)$ Å, $V = 6370.4(6)$ Å$^3$, space group $R\bar{3}$, hexagonal setting, $Z = 3$, $T = 100$ K, 133163 reflections measured, 2737 unique ($R_{int} = 0.0367$), final $R1 = 0.0445$, $wR2 = 0.1224$ for 2277 observed reflections [$I > 2\sigma(I)$].
[31] J. Vicente, M. T. Chicote, I. Saura-Llamas, P. G. Jones, K. Meyer-Bäse, C. F. Erdbrügger, *Organometallics* **1988**, *7*, 997–1006.
[32] E. J. Fernández, M. C. Gimeno, A. Laguna, J. M. López-de-Luzuriaga, M. Monge, P. Pyykkö, D. Sundholm, *J. Am. Chem. Soc.* **2000**, *122*, 7287–7293.
[33] E. J. Fernández, A. Laguna, J. M. López-de-Luzuriaga, M. Monge, M. E. Olmos, M. Rodríguez-Castillo, *Organometallics* **2006**, *25*, 3639–3646.
[34] A. Purath, C. Dohmeier, A. Ecker, R. Köppe, H. Krautscheid, H. Schnöckel, R. Ahlrichs, C. Stoermer, J. Friedrich, P. Jutzi, *J. Am. Chem. Soc.* **2000**, *122*, 6955–6959.
[35] M. Huber, J. Hartig, K. Koch, H. Schnöckel, *Z. Anorg. Allg. Chem.* **2009**, *635*, 423–430.
[36] Y. Wang, H. F. Su, C. F. Xu, G. Li, L. Gell, S. C. Lin, Z. C. Tang, H. Häkkinen, N. F. Zheng, *J. Am. Chem. Soc.* **2015**, *137*, 4324–4327.
[37] Y. Wang, X. K. Wan, L. T. Ren, H. F. Su, G. Li, S. Malola, S. C. Lin, Z. C. Tang, H. Häkkinen, B. K. Teo, Q. M. Wang, N. F. Zheng, *J. Am. Chem. Soc.* **2016**, *138*, 3278–3281.
[38] M. W. Heaven, A. Dass, P. S. White, K. M. Holt, R. W. Murray, *J. Am. Chem. Soc.* **2008**, *130*, 3754–3755.
[39] Y. Negishi, W. Kurashige, Y. Niihori, T. Iwasa, K. Nobusada, *Phys. Chem. Chem. Phys.* **2010**, *12*, 6219–6225.
[40] H. F. Qian, D. E. Jiang, G. Li, C. Gayathri, A. Das, R. R. Gil, R. C. Jin, *J. Am. Chem. Soc.* **2012**, *134*, 16159–16162.
[41] C. P. Joshi, M. S. Bootharaju, M. J. Alhilaly, O. M. Bakr, *J. Am. Chem. Soc.* **2015**, *137*, 11578–11581.
[42] J. Z. Yan, H. F. Su, H. Y. Yang, S. Malola, S. C. Lin, H. Häkkinen, N. F. Zheng, *J. Am. Chem. Soc.* **2015**, *137*, 11880–11883.

Received: September 18, 2016
Revised: October 9, 2016
Published online: November 3, 2016

  